General Disclaimer

One or more of the Following Statements may affect this Document

- This document has been reproduced from the best copy furnished by the organizational source. It is being released in the interest of making available as much information as possible.

- This document may contain data, which exceeds the sheet parameters. It was furnished in this condition by the organizational source and is the best copy available.

- This document may contain tone-on-tone or color graphs, charts and/or pictures, which have been reproduced in black and white.

- This document is paginated as submitted by the original source.

- Portions of this document are not fully legible due to the historical nature of some of the material. However, it is the best reproduction available from the original submission.

NASA TECHNICAL MEMORANDUM

NASA TM X-73690

NASA TM X-73690

(NASA-TM-X-73690) OPTIMIZATION OF CONFINEMENT IN A TOROIDAL PLASMA SUBJECT TO STRONG RADIAL ELECTRIC FIELDS (NASA) 33 p HC A03/MF A01 CSCL 20I

N77-27919

G3/75

Unclas 35465

OPTIMIZATION OF CONFINEMENT IN A TOROIDAL PLASMA SUBJECT TO STRONG RADIAL ELECTRIC FIELDS

by J. Reece Roth
Lewis Research Center
Cleveland, Ohio 44135

TECHNICAL PAPER presented at the
International Conference on Plasma Science
sponsored by the Institute of Electrical and Electronics Engineers
Troy, New York, May 23-25, 1977

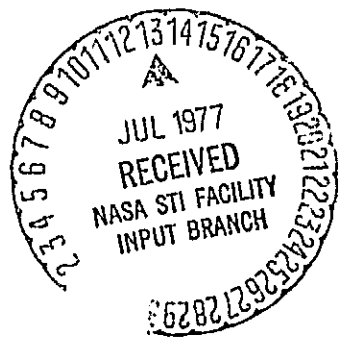

OPTIMIZATION OF CONFINEMENT IN A TOROIDAL PLASMA SUBJECT TO STRONG RADIAL ELECTRIC FIELDS

by J. Reece Roth

National Aeronautics and Space Administration
Lewis Research Center
Cleveland, Ohio 44135

E-9225

ABSTRACT

The toroidal ring of plasma contained in the NASA Lewis Bumpy Torus facility may be biased to positive or negative potentials approaching 50 kilovolts by applying DC voltages of the respective polarity to 12 or fewer midplane electrode rings. The radial electric fields, which are responsible for raising the ions to high energies by ExB/B^2 drift, then point out of or into the plasma. This paper is a preliminary report on the identification and optimization of independent variables which affect the ion density and confinement time in the NASA Lewis Bumpy Torus plasma. The independent variables include the polarity, position, and number of the midplane electrode rings, the method of gas injection, and the polarity and strength of a weak vertical magnetic field. Some characteristic data taken under conditions when most of the independent variables were optimized are presented. The highest value of the electron number density on the plasma axis is 3.2×10^{12}/cc, the highest ion heating efficiency is 47 percent, and the longest particle containment time is 2.0 milliseconds.

INTRODUCTION

Pure magnetic containment, in which a plasma is confined solely by strong magnetic fields, has been the dominant approach since the beginning of controlled fusion research. Externally applied electric fields have not thus far played a role in toroidal plasma confinement. An experiment to electrostatically confine oscillating ions to a small volume was reported by Hirsch (ref. 1). Several investigators have applied strong electric fields to a plasma in cusp (refs. 2 and 3) or mirror (refs. 4 and 5) magnetic geometries to enhance plasma

STAR Category 75

confinement. Theoretical papers by Kovrizhnykh (refs. 6 and 7) and Stix (refs. 8 and 9) have examined the confinement implications of ambipolar electric fields in toroidal geometries. There does not appear to be relevant literature on the subject of imposed, non-ambipolar electric fields in toroidal geometries.

The steady-state plasma in the NASA Lewis Bumpy Torus Facility is generated by a modified Penning discharge operated in conjunction with the Bumpy Torus magnetic field geometry. The NASA Lewis Bumpy Torus Experiment possesses four distinguishing characteristics:

1. The plasma, magnetic field, and ion heating mechanism are operated in the steady state.

2. The ion kinetic temperature is typically a factor of 10 to 100 higher than the electron temperature.

3. The plasma is acted on by a combination of strong DC magnetic and electric fields.

4. The necessary fusion technology is being developed in parallel with the physics, particularly, superconducting magnet technology and cryogenic and high voltage techniques.

The Bumpy Torus magnet facility is described in detail elsewhere (refs. 10 and 11) and consists of 12 superconducting coils equally spaced around a toroidal volume 1.52 meters in major diameter. An isometric cutaway drawing of the Bumpy Torus plasma is shown in figure 1. Each coil has a minor diameter of 19 centimeters, and the maximum designed magnetic field on the magnetic axis is 3.0 tesla. The minimum magnetic field on the magnetic axis between coils is 40 percent of the maximum magnetic field. The coil array is located in a single vacuum tank 2.6 meters in major diameter.

Previous investigations (refs. 12 to 17) have shown that, in common with Penning discharges and magnetron-like devices, the plasma forms rotating spokes which gyrate around the minor circumference of the plasma with velocities comparable to the E/B drift velocity; and the ions of these rotating spokes then form an energy reservoir which is thermalized to the high kinetic temperatures observed. The presence of strong radial electric fields acting on the plasma, which usually exceed values of 1 kilovolt per centimeter, not only is responsible for raising the ions to energies on the order of kilovolts, but also affects the containment of the plasma. It was shown (refs. 16 and 17) that the plasma number density and confinement time can increase more than an order of magnitude if the electric field acting along the minor radius of the toroidal plasma points inward, relative to the values observed when it points (and pushes ions) radially outward.

This paper is a preliminary report on the identification and optimization of 12 independent variables which affect the ion density and containment time in the NASA Lewis Bumpy Torus plasma. Their influence on the plasma properties is discussed. Complete information about the optimum values and functional dependence of all 12 independent variable is not yet available. Some characteristic data taken under conditions when most of the independent variables were optimized are presented. These include the highest plasma number density, the highest ion heating efficiency, and the longest particle containment time observed so far in this experiment.

INFLUENCE OF INDEPENDENT VARIABLES ON PLASMA CHARACTERISTICS

The NASA Lewis Bumpy Torus experiment appears to be the first instance in which a strong radial electric field is deliberately imposed on a toroidal plasma. The uniqueness of this approach and the absence of prior literature has made it necessary to undertake a systematic program to identify the independent variables which influence the plasma characteristics of interest. The dependent variables include ion kinetic temperature, number density, and containment time, as well as the electrode current drawn by the power supply. The current status of this research program is summarized in table I. The 12 independent variables which have been found to influence the plasma characteristics are listed on the left. Whether they have a strong, weak, or no influence on the plasma characteristics is indicated in the respective columns. In some cases, the influence of an independent variable has not yet been systematically measured or its functional dependence clarified, and in these cases a question mark has been entered in the table. The entries in table I are a gross oversimplification of a situation which is often complex, but they do indicate the relative importance of the independent variables on particular plasma characteristics. The dependences listed in the bottom six rows of table I are entered on the assumption that the other independent variables are at or near their optimum values, in terms of obtaining the highest possible plasma temperatures, number densities, and containment times. The influence of the first six independent variables listed in table I have been covered in part in previous publications (refs. 12 to 18). These previous data were often taken under conditions that were far from optimized, and some of them have now been extended with new data taken under

conditions in which more of the independent variables listed on table I have been adjusted to their optimum values. The effects of the last six independent variables on table I have not been previously reported, and additional work remains to be done in separating out their interrelations and in the determination of their optimum values.

An empirical correlation incorporating the first five independent variables listed on table I was obtained in reference 18 and yielded the scaling laws stated in equations (1) to (3).

$$I_p = D_1 V_A^{1.10} p_o^{1.50} B_{max}^{0.25} \text{ amps} \tag{1}$$

$$T_i = C_2 V_A^{0.70} B_{max}^{0.30} \text{ eV} \tag{2}$$

$$n_e = C_3 V_A^{1.10} p_o^{0.40} / \text{cm}^3 \tag{3}$$

These scaling laws held over one order of magnitude in the ion temperature, three orders of magnitude in plasma current, and three orders of magnitude in the electron number density. These scaling laws did not exhibit a knee or other asymptotic phenomena up to the upper limit of their range. In this correlation study, it was found that the constants which multiply these scaling laws depended on the mode of plasma operation and the polarity of the midplane electrode rings, as follows.

$$D_1 = \begin{cases} 3.8\times10^{-4} \text{ A}/(\mu\text{T})^{1.5}(\text{kV})^{1.1}(\text{T})^{0.25} & \text{HPM} \quad + \\ 1.5\times10^{-4} \text{ A}/(\mu\text{T})^{1.5}(\text{kV})^{1.1}(\text{T})^{0.25} & \text{LPM} \quad + \\ 3\times10^{-4} \text{ A}/(\mu\text{T})^{1.5}(\text{kV})^{1.1}(\text{T})^{0.25} & \text{Both} \quad - \end{cases}$$

$$C_2 = 160 \text{ eV}/(\text{kV})^{0.70}(\text{T})^{0.3} \qquad \text{Both} \quad \text{Both}$$

$$C_3 = \begin{cases} 2.2\times10^{9} \\ \qquad \text{cm}^{-3}/(\text{kV})^{1.1}(\mu\text{T})^{0.40} & \text{Both} \quad + \\ 5.5\times10^{8} & \qquad\quad - \end{cases}$$

These scaling laws were obtained when there were midplane electrode rings in all 12 sectors, and also under conditions for which the last six independent variables in table I were not optimized.

From equation (1) it is evident that the electrode current is a strong function of the electrode voltage and the neutral gas pressure, and only weakly dependent on the magnetic field. The constant D_1 which multiplied equation (1) depends both on the mode of operation and the polarity of the midplane electrode rings. From equation (2) it is evident that the ion kinetic temperature has a strong dependence on electrode voltage, a weak dependence on magnetic field strength, and does not depend on the background neutral gas pressure. The constant C_2 multiplying equation (2) is independent of the mode of operation and the polarity of the electrode rings, and the ion kinetic temperature therefore does not depend on these independent variables. The scaling law of equation (3) for the electron number density has a strong dependence on electrode voltage, a weak dependence on neutral gas pressure, and no dependence on the magnetic field strength. Subsequent measurements under more nearly optimized conditions indicate that the plasma number density does have a weak dependence on the magnetic field strength. The constant C_3 which multiplies the scaling law for electron number density depends on the polarity of the electrode rings. Subsequent measurements made under optimized conditions have shown that the plasma number density has a strong dependence on the mode of plasma operation.

In reference 18 a scaling law was not explicitly obtained for the particle confinement time. In references 16 and 17 it has been shown that the particle containment time may be calculated from the average particle number density and the total electrode current according to the following expression:

$$\tau_p = \frac{n_e e V_p}{I_p} \tag{4}$$

If one substitutes equation (1) for the electrode current and equation (3) for the electron number density equation equation (4), the predicted functional dependence of the particle confinement time is equal to:

$$\tau_p = \frac{eV_p C_3}{D_1} \frac{1}{p_o^{1.10} B_{max}^{0.25}} = \frac{D_2}{p_o^{1.10} B_{max}^{0.25}} \tag{5}$$

where the constant D_2 depends on both the mode of operation and the polarity of the electrode rings. Equation (5) predicts that the particle confinement time is a strong function of the background neutral gas pressure, a weak function of magnetic field strength, and is independent of the electrode voltage. There is a strong dependence of the constant D_2 on the mode of operation and the polarity of the midplane electrode rings. These functional dependences are consistent with data described later in this report, although it has been found that the particle confinement time is independent of electrode voltage only when the radial and vertical alignment of the electrode rings are near the optimum value.

The effect of varying the number and configuration of the midplane electrode rings was examined in reference 16, and in subsequent unpublished research. It was found that if all other independent variables remain the same, the ion kinetic temperature is only weakly dependent on the number of midplane electrode rings, the total electrode current increases as the number of midplane electrode rings is decreased, and the plasma number density and confinement time increase as the number of electrode rings is reduced.

Electrode Ring Alignment

On figure 2 is shown a schematic drawing of the electric field surrounding the Bumpy Torus plasma when the electrode rings bias the entire toroidal ring of plasma to high negative potentials. The electric field is strongest between the grounded magnet dewars and the plasma itself. It is this radial electric field which raises the ions to high E/B drift velocities, and is responsible for heating the plasma. When the electric field points inward, the density and containment times are approximately a factor of 10 larger than they are when the electrode rings are positive with the electric field pointing away from the plasma (refs. 41 and 15). A similar effect is apparent in the data presented in this report.

It has been found that precise alignment of the plasma, along the major radius of the torus and in the vertical direction, has an extremely important effect on containment. This sensitivity to alignment exists for reasons which are illustrated by figure 3. Figure 3 shows a plan view of the plasma and magnetic field lines in the equatorial plane of the torus, and the location of a typical midplane electrode ring. For positive polarities, the plasma tends to be confined within magnetic field lines which intersect the inside diameter of the electrode ring. If the electrode ring is aligned with its center on the geometric

center of the containment volume, the toroidicity of the plasma will result in a stronger electric field on the inside radius of the plasma than will occur on the outside radius as it passes through the grounded magnet dewars.

The ions and electrons drift azimuthally about the minor circumference of the plasma as a result of the crossed electric and magnetic fields. When the electric field along the minor radius of the plasma is azimuthally asymmetric, the rotating particles will experience a net electric field, which points radially inward for the case shown in figure 3. The situation depicted on figure 3 will result in a drift of particles out of the plane of the paper to the upper surface of the plasma volume. Under conditions illustrated in figure 3, it has been observed in the laboratory that the plasma drifts to the top of the containment volume. As a result, the upper boundary of the plasma is more luminous and has a sharper edge than the lower surface.

The net electric field along the major radius of the torus can be adjusted by moving the electrode rings radially inward or outward. In the case shown in figure 3, it is clear that if the electrode rings are moved radially outward, away from the geometric center of the containment volume, there will exist a position for which there will be no net radial electric field along the major radius of the torus, and the electric field drifts will then be minimized.

A similar situation exists if the electrode is vertically misaligned, above or below the equatorial plane. If the center of the electrode ring is above the equatorial plane, there will be a net electric field pointing vertically upward, and the plasma will tend to drift outward along a major radius. These residual electric field drifts are very damaging to plasma confinement, because they cause equal rates of loss of both species of charge.

In order to assess the effect of vertical and radial misalignment on plasma containment, two of the 12 midplane electrode rings, in sectors 5 and 6, were outfitted with a movable support, which made it possible to move them over a total distance of 9 centimeters along the major radius. At the same time, provision was made to adjust the same two electrode rings vertically over a total distance of 5 centimeters, in increments of 2.5 millimeters. All data reported below were taken in a deuterium plasma, with round electrode rings, with a maximum magnetic field of 2.4 tesla (1.0 tesla at the midplane), and with only electrodes 5 and 6 in place.

On figures 4 and 5 are shown plots of the number density and confinement time, respectively, as functions of the position of electrodes 5 and 6 along the major radius of the toroidal containment volume. The containment time was calculated using equation (4) as derived in references 16 and 17. The solid

symbols refer to the low pressure mode of operation, the open symbols to the high pressure mode, and both electrode ring polarities are shown. The optimum radial position is about 120 millimeters for the two modes of operation with positive electrode polarity and is about 93 millimeters for both modes with negative polarity. The optimum value for the negative polarity is displaced 37 millimeters further in toward the major axis of the torus than is the optimum value for positive polarity. This apparently occurs because with positive polarities the plasma fills the entire confinement volume defined by the electrode ring boundaries, but with negative polarities, the plasma cross section has a shape of the letter D, characteristic of magnetic field dominated drift surfaces, with the flat side on the inner major radius of the confinement volume. This flat inner side of the plasma is somewhat further out along the major radius than is the boundary of the plasma created with positive polarities, and moves along the major radius in response to the value of the weak vertical magnetic field applied to the plasma. On figures 4(b) and 5(b), it is evident that the plasma with negative electrode polarity is extinguished if it is too far from its optimum radial alignment.

In figures 6 and 7 are plotted the number density and confinement time, respectively, as functions of the vertical displacement above or below the equatorial plane. For these data, the radial positions were adjusted to the optimum values appropriate to each polarity. For positive polarity, the plasma confinement is optimized when the centers of the electrode rings are aligned on the equatorial plane of the torus. For negative polarities, confinement is optimized when the electrode rings are above the equatorial plane by an amount which depends on the mode of operation. In the high pressure mode of operation with negative electrode polarity, the plasma is extinguished if the vertical alignment to too far off optimum.

Method of Neutral Gas Injection

In reference 16 it was shown that the current drawn by an individual electrode ring will increase if a jet of neutral deuterium gas is injected locally in that sector. The base pressure of the Bumpy Torus facility is about 6×10^{-8} torr, and the operating pressures, generally in the range of 0.4 to 10×10^{-5} torr, are maintained by a constant flow of deuterium gas through the vacuum system. This facility has been operated in the past by injecting the incoming deuterium gas vertically upward along the major axis of the torus. This symmetric injection

of the neutral gas results in background neutral gas densities that are the same in every sector.

The plasma is sustained by electron-neutral impact ionization of the background gas, but energetic ions also are charge-exchanged on the molecular deuterium gas and lost to the walls. At particle densities on the order of 10^{12}/cubic centimeters, the mean-free path of the neutral deuterium molecules becomes comparable to the plasma diameter, and the neutral density inside the containment volume can become substantially less than that of the background gas in the rest of the vacuum tank. Under these conditions, it becomes possible to inject neutral gas across a minor diameter of the confinement volume, or tangentially to the confined volume, and thereby decouple the plasma number density from the background neutral number density in the confinement volume outside this neutral gas jet. Under such conditions, the majority of ionizations would occur in the neutral gas jet, and a higher plasma density can be sustained with a lower neutral number density in the remainder of the plasma. This would substantially reduce the level of charge-exchanged energy losses in the confinement volume.

To test the effects of the method of neutral gas injection, a comparison was made in which the neutral gas was injected vertically upward along the major axis of the tank, across the minor diameter of the containment volume, and tangentially to the containment volume. The radial and tangential gas injectors were located in sector 10, in which the microwave interferometer was located. These are illustrated schematically on figure 8. On figures 9 and 10 are shown plots of the ion number density and containment time for both electrode polarities as functions of electrode voltage, for the high and low pressure modes of operation, and for the three methods of injecting neutral gas. In virtually all cases, the number density and containment times were greatest when the neutral gas jet was injected tangentially to the containment volume, thus allowing a maximum opportunity for the incoming neutral gas to interact with the plasma.

Effects of Polarity and Strength of Vertical Magnetic Field

The vacuum tank of the NASA Lewis Bumpy Torus facility (shown in fig. 1) has a major diameter of 2.6 meters. Wound on the outside surface of this vacuum tank are two air-cooled copper coils which are symmetrically located 0.43

meter above and below the equatorial plane of the confinement volume. These coils can generate a steady-state, weak vertical magnetic field up to 70 gauss on the axis of the containment volume, the polarity of which can point either upward or downward. The purpose of adding a weak vertical magnetic field is to compensate for possible magnetic field errors of a kind discussed by Sprott (ref. 19), and which can arise in this facility from the current loop formed in the lower liquid helium manifold by series connection of the 12 superconducting coils. In the experiment reported by Dandl, et al. (ref. 20) a weak vertical magnetic field considerably improved the stability and confinement of the ELMO Bumpy Torus plasma.

On figures 11 and 12 are shown the ion number density and containment time plotted as functions of the vertical magnetic field. Negative values of the vertical field point downward, and positive values point upward. The plasma number density and confinement time are surprisingly sensitive to such a small force acting on the plasma. For the negative electrode data on figure 11(b), increasing the vertical magnetic field from zero to 16 gauss increases the confined density by a factor of four. The optimum vertical magnetic field seems not to depend on the plasma number density or mode of operation; it is +5 gauss for positive polarities and +16 gauss for negative polarities. When the plasma densities were above 10^{12}/cubic centimeter, the optimum magnetic field for negative polarity decreased slightly to 13 gauss. Between 20 and 30 gauss, no plasma could be generated with negative polarity, and only a weak background plasma existed with positive polarity. The particle containment times shown in figures 12(a) and (b) are not as sensitive as the density to the vertical magnetic field.

The physical mechanism responsible for this extreme sensitivity to the vertical magnetic field is not clear. The 500 ampere current loop in the lower liquid helium manifold creates a vertical magnetic field which points downwards, but is only 3.2 gauss on the axis of the containment volume. Its magnitude is apparently not great enough to account for the optimum vertical fields observed, nor for the curious fact that a change of only 6 gauss on figure 11(b) will change from an optimum plasma density to no plasma at all. Visual observation of the plasma, by looking vertically downward from a glass viewport on the top of the vacuum tank, showed that as the vertical magnetic field was varied from zero to positive values, the plasma expanded inward along a major radius until the plasma contacted the inner edges of the superconducting coil shields. After this point, the plasma density decreased and finally quenched at about 25 gauss.

CHARACTERISTIC OPTIMIZED EXPERIMENTAL DATA

The apparatus was adjusted so that all of the independent variables investigated to date were set at their optimum values. The average electron number density (the maximum density on the axis is twice this) and the particle containment time are plotted as functions of the electrode current on figures 13(a) and (b). Data are shown for two values of neutral gas pressure. These results are encouraging in that the density is proportional to electrode current, and the confinement time is virtually constant. The density and the confinement time are both higher for the higher neutral background gas pressure. The density is a very rapidly increasing function of electrode voltage in this mode of operation (see fig. 9(b)).

CONCLUDING REMARKS

Obtaining the best possible performance from the electric field Bumpy Torus has proven to be a complicated optimization procedure involving the 12 independent variables which are listed on table I. The desirable trends for most of these variables are now generally understood. The desirable conditions listed in table I represent an optimum for some of the variables, but it cannot be ruled out that additional local optima might exist under entirely different sets of operating conditions. It may never be possible to guarantee that the conditions listed in the last column of table I are also a global optimum for the operation of the electric field Bumpy Torus. The question marks listed in table I represent functional dependences which have not as yet been examined in enough detail to report in this preliminary paper.

Future work will require investigation of the remaining independent variables and obtaining definitive scaling laws for the behavior of the fusion-related dependent variables as functions of the primary independent variables.

REFERENCES

1. R. L. Hirsch, J. Appl. Phys., 38, 4522 (1967).

2. A. A. Ware, and J. E. Faulkner, Nucl. Fusion, 9, 353 (1969).

3. B. L. Stansfield, et al., Can. J. Phys., 54, 1856 (1976).

4. R. W. Moir, W. L. Barr, and R. F. Post, Phys. Fluids, 14, 2531 (1971).

5. Y. Nishida, S. Kawamata, and K. Ishii, Institute of Plasma Physics. Report IPPJ-256, Nagoya, Japan (1976).

6. L. M. Kozrizhnykh, Sov. Phys., JETP, 29, 475 (1969).

7. L. M. Kovrizhnykh, Sov. Phys., JETP, 35, 709 (1972).

8. T. H. Stix, Phys. Fluids, 14, 702 (1971).

9. T. H. Stix, Phys. Fluids, 14, 702 (1971).

10. J. R. Roth, et al., NASA TN D-7353 (1973).

11. J. R. Roth, et al., Fifth Applied Superconductivity Conference, p. 361, (Inst. Elect. Electron. Eng., New York, 1972).

12. J. R. Roth, G. A. Gerdin, and R. W. Richardson, NASA TN D-8114 (1976).

13. J. R. Roth, G. A. Gerdin, and R. W. Richardson, IEEE Trans. Plasma Sci., PS-4, 166 (1976).

14. J. R. Roth, and G. A. Gerdin, NASA TN D-8211 (1976).

15. J. R. Roth, and G. A. Gerdin, Plasma Phys., 19, 423-446, 1977.

16. J. R. Roth, NASA TN D-8466 (1977).

17. J. R. Roth, "Effects of Applied D. C. Radial Electric Fields on Particle Transport in a Bumpy Torus Plasma" (to be published).

18. J. R. Roth, NASA TM X-73434 (1976).

19. J. C. Scott, Phys. Fluids, 16, 1157 (1973).

20. R. A. Dandl, R. A. Bary, and H. E. Eason, Oak Ridge National Laboratory Tech. Memo. 4941, Oak Ridge, Tenn. (1975).

TABLE I. - INFLUENCE OF INDEPENDENT VARIABLES ON PLASMA CHARACTERISTICS

Number	Independent variable	Dependent variable				Desirable operating condition
		Ion kinetic temperature	Plasma number density	Particle confinement time	Electrode current	
1	Electrode voltage	Strong	Strong	None	Strong	As high as possible
2	Background neutral gas pressure	None	Weak	Strong	Strong	$4.0 - 9.0 \times 10^{-5}$ torr
3	Magnetic field strength	Weak	Weak	Weak	Weak	
4	Mode of plasma operation	None	Strong	Strong	Strong	High pressure mode
5	Polarity of midplane electrode rings	None	Strong	Strong	Strong	Negative electrode polarity
6	Number of midplane electrode rings	Weak	Strong	Strong	Strong	Two electrode rings
7	Electrode ring shape	?	?	?	?	
8	Radial alignment of electrode rings	?	Strong	Strong	Strong	Optimum depends on polarity
9	Vertical alignment of electrode rings	?	Strong	Strong	Strong	On equatorial plane
10	Method of neutral gas injection	None	Weak	Weak	Weak	Tangential gas injection
11	Polarity of vertical magnetic field	?	Strong	Strong	Strong	Magnetic field pointing upwards
12	Strength of vertical magnetic field	?	Strong	Strong	Strong	Optimum depends on polarity

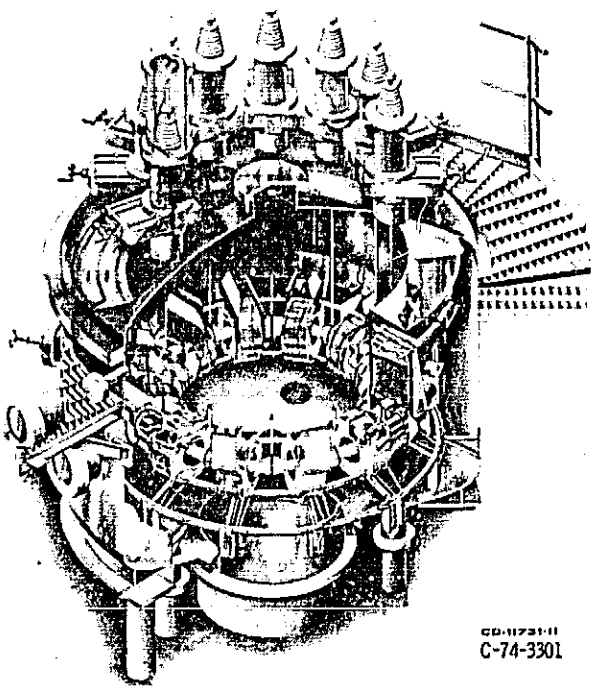

Figure 1. - Isometric cutaway drawing of NASA Lewis bumpy-torus superconducting magnet facility.

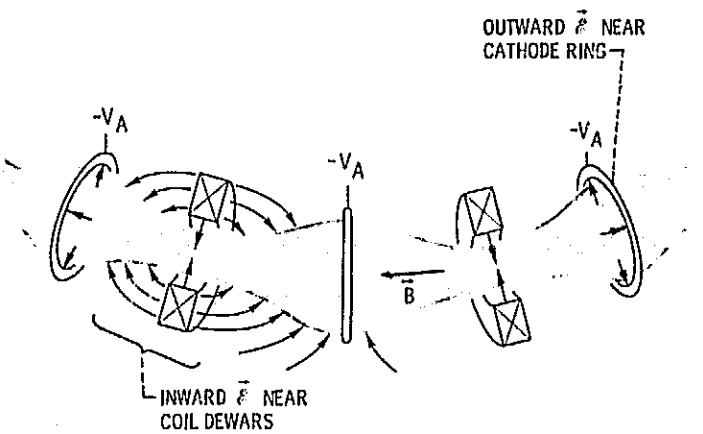

Figure 2. - Electric field structure in bumpy torus with negative midplane electrodes.

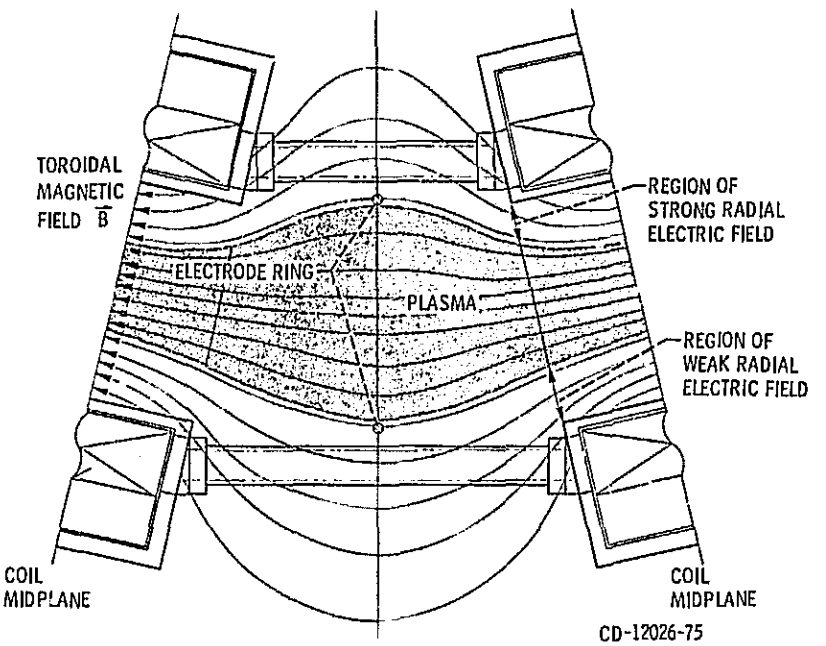

Figure 3. - Toroidicity of electric field.

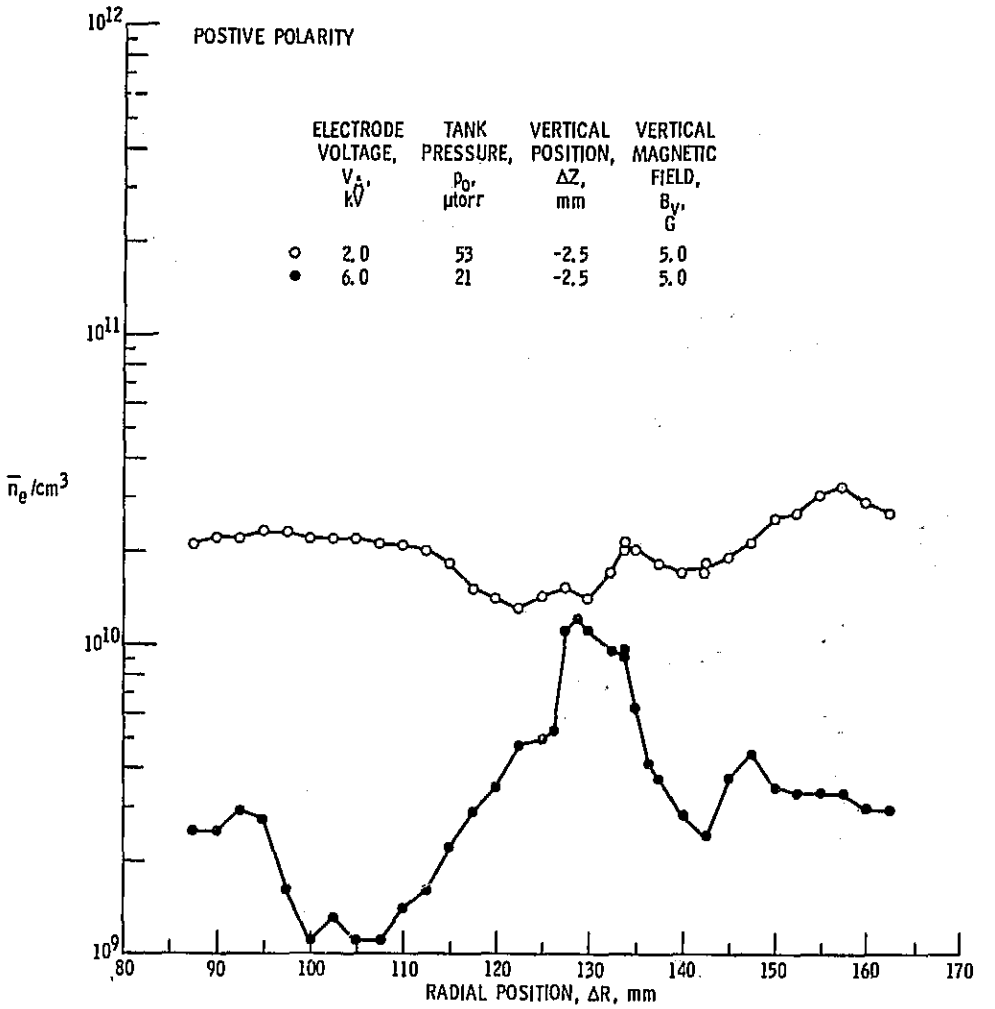

(a) POSITIVE POLARITY.

Figure 4. - Particle density as a function of radial alignment of electrode rings.

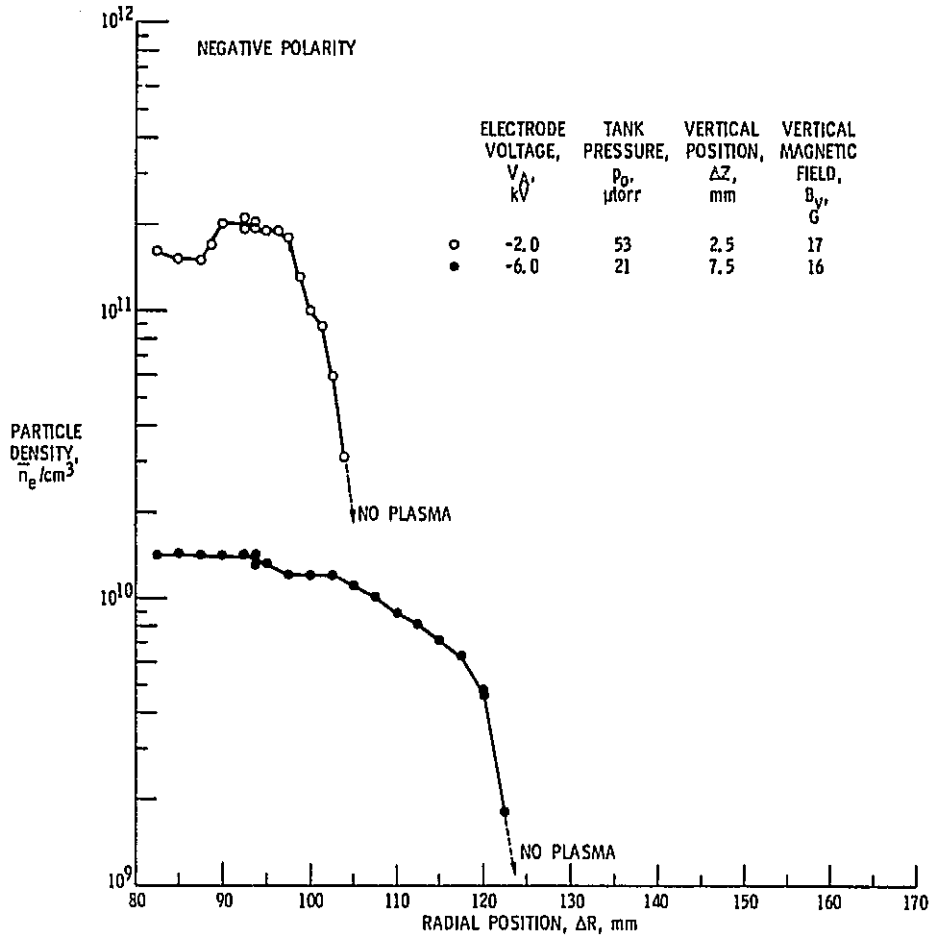

(b) NEGATIVE POLARITY.

Figure 4. - Concluded.

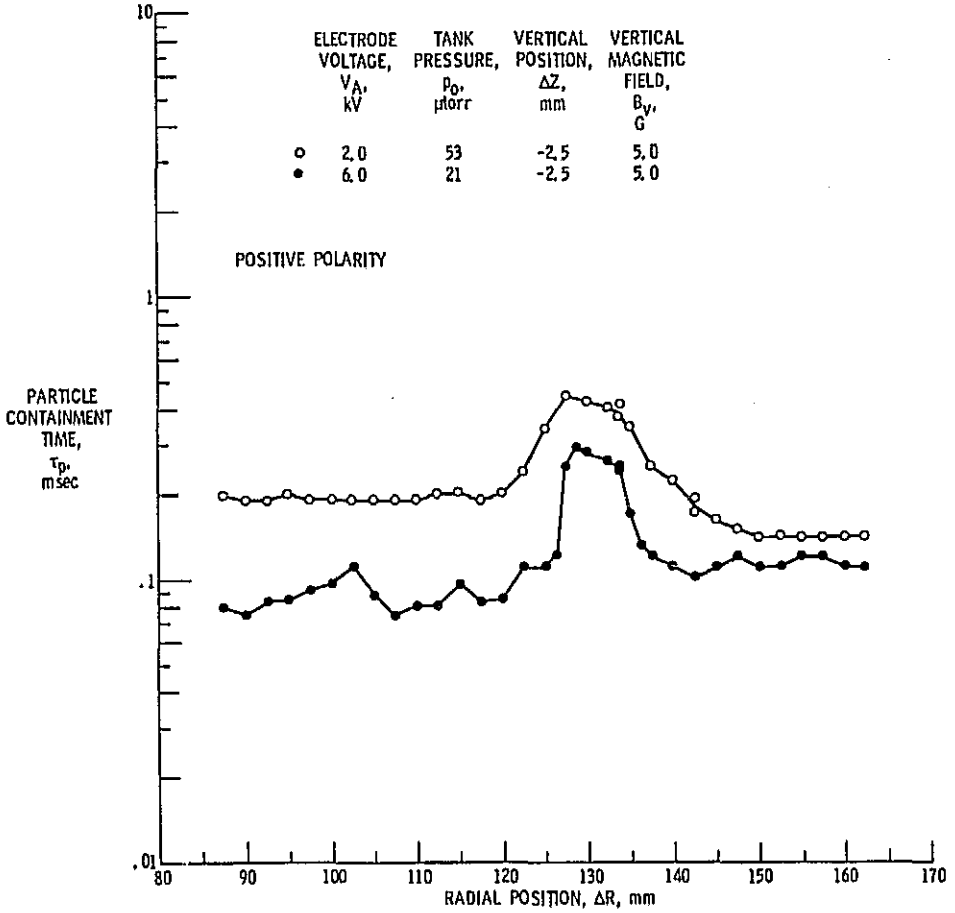

(a) POSITIVE POLARITY.

Figure 5. - Particle containment time as a function of radial position of electrode rings for same conditions as figure 4.

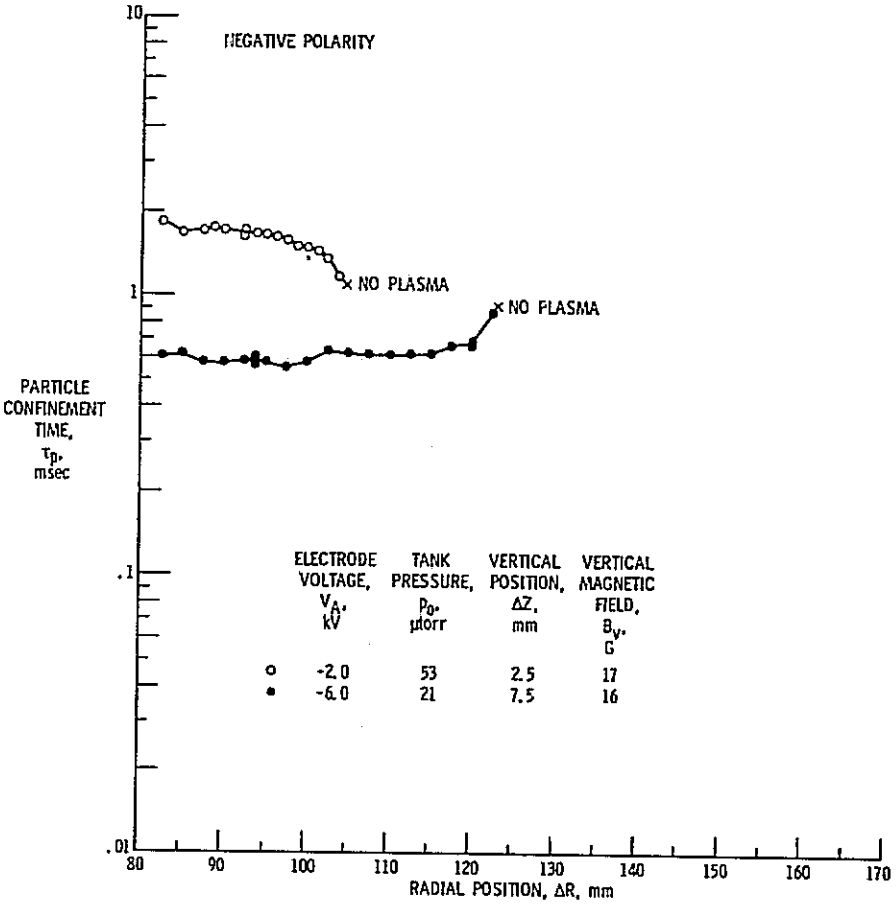

(b) NEGATIVE POLARITY.

Figure 5. - Concluded.

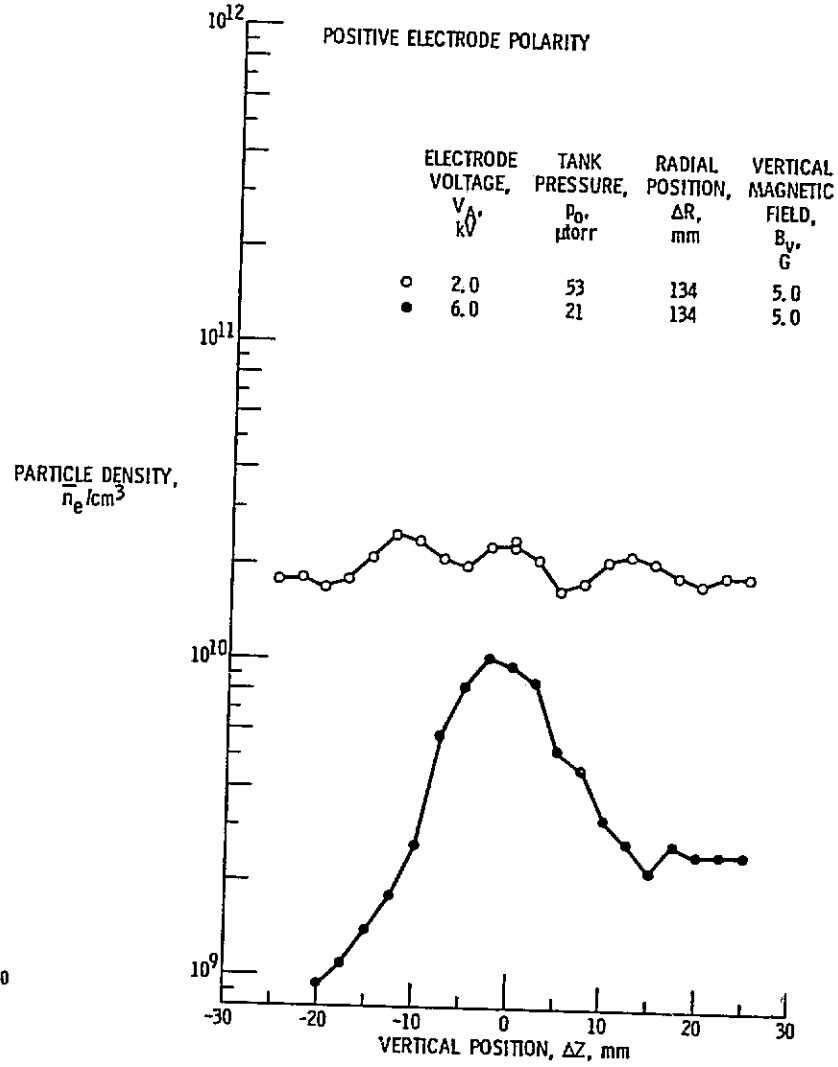

(a) POSITIVE POLARITY.

Figure 6. - Average particle number density as a function of vertical position of electrode rings relative to equatorial plane of plasma.

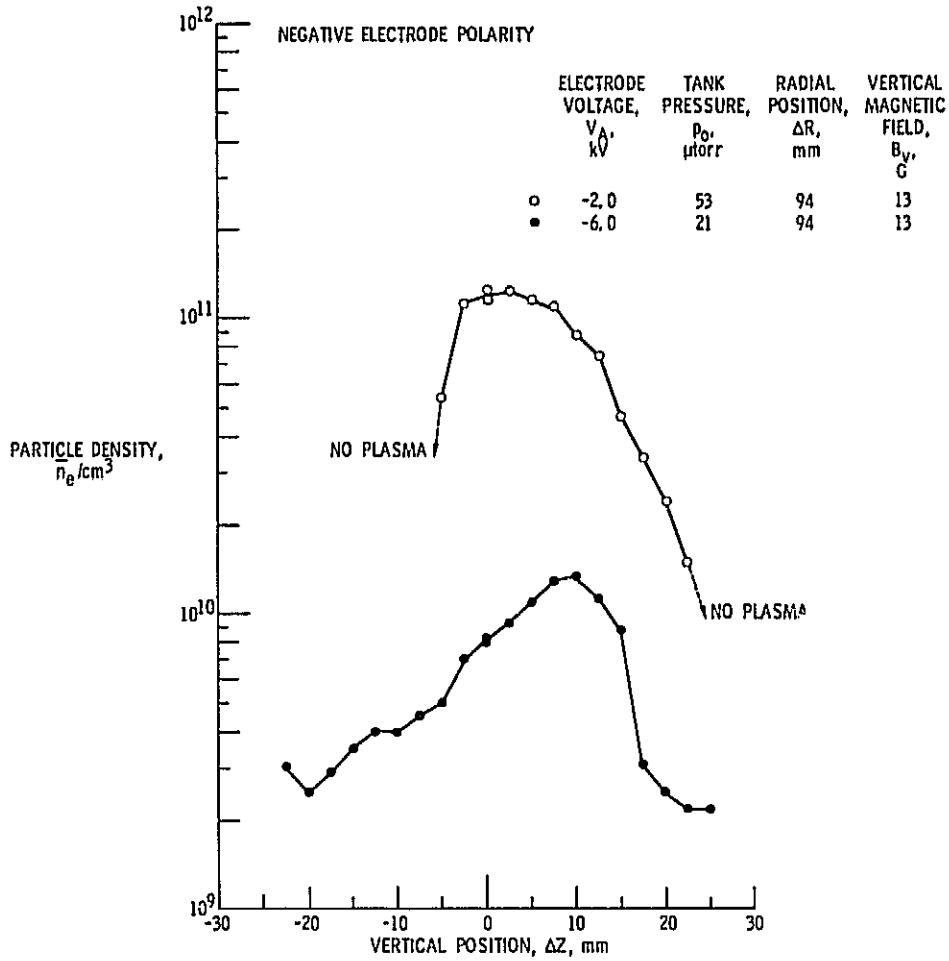

(b) NEGATIVE POLARITY.

Figure 6. - Concluded.

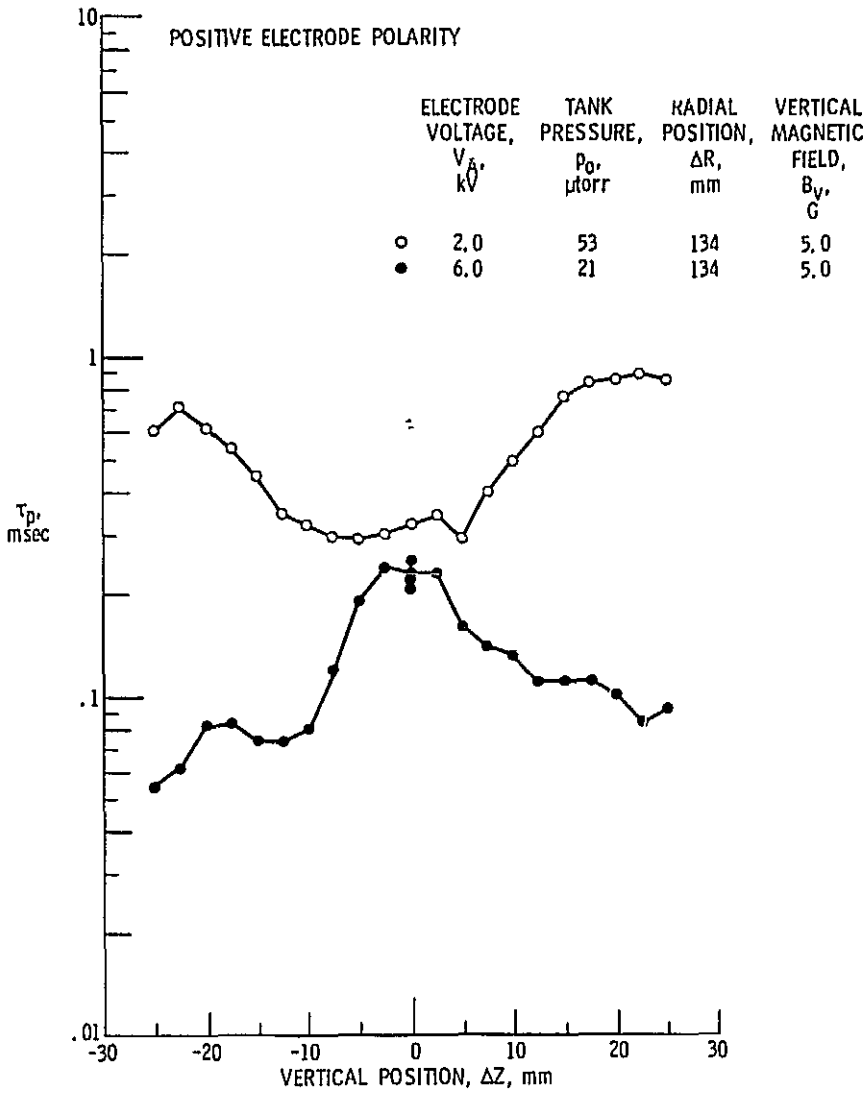

(a) POSITIVE POLARITY.

Figure 7. - Particle containment time as a function of vertical position of electrode rings for same conditions as figure 6.

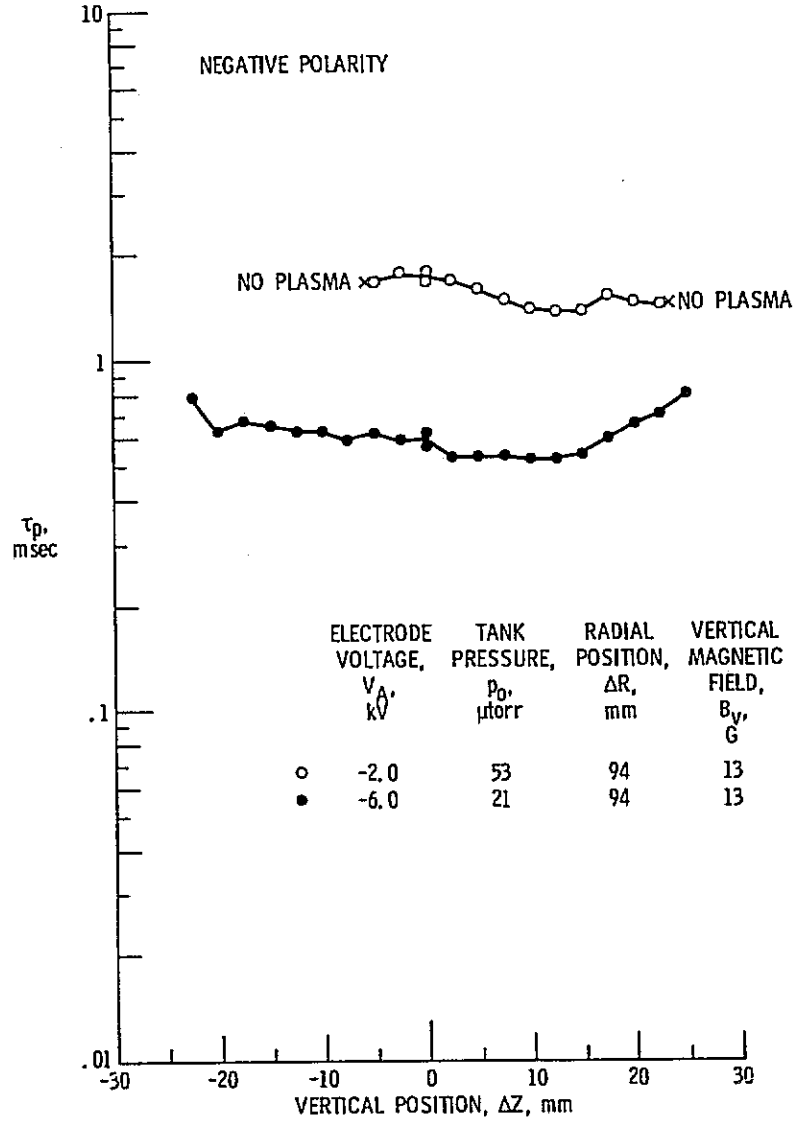

(b) NEGATIVE POLARITY.

Figure 7. - Concluded.

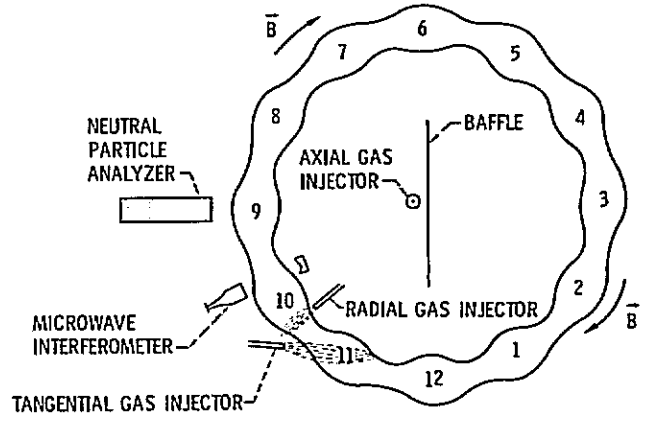

Figure 8. - Location of instruments and neutral gas injectors in toroidal array.

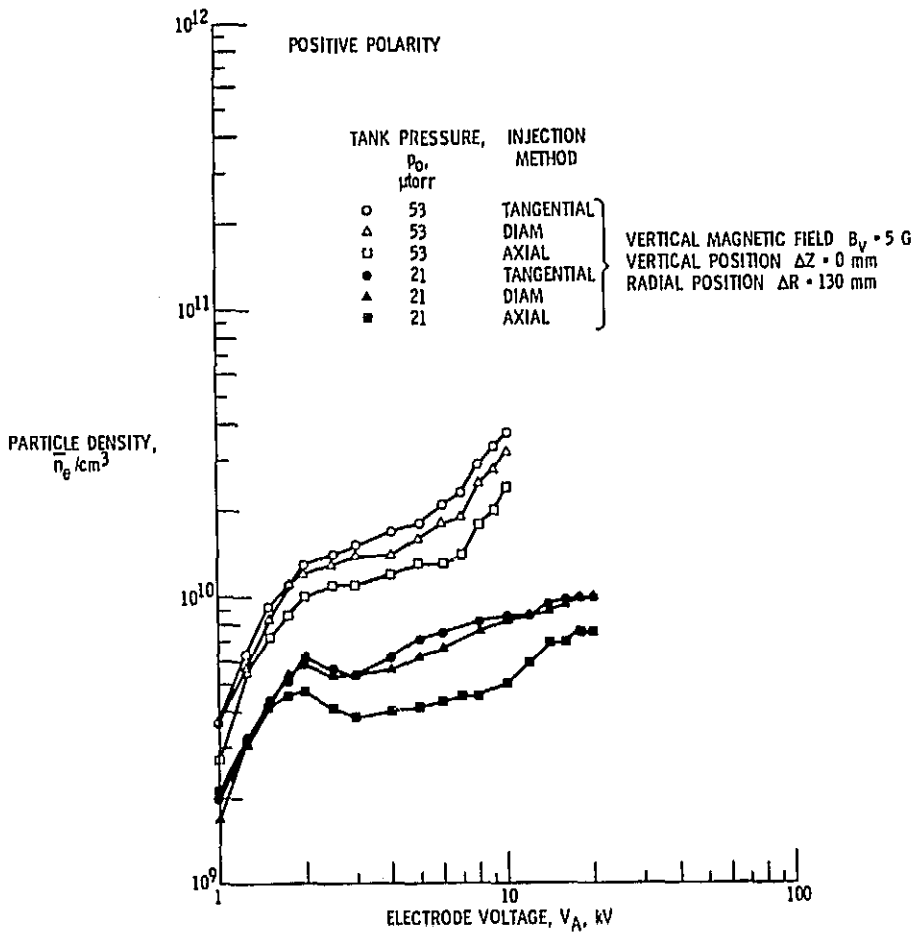

(a) POSITIVE POLARITY.

Figure 9. - Average particle number density as a function of electrode voltage for three methods of neutral gas injection.

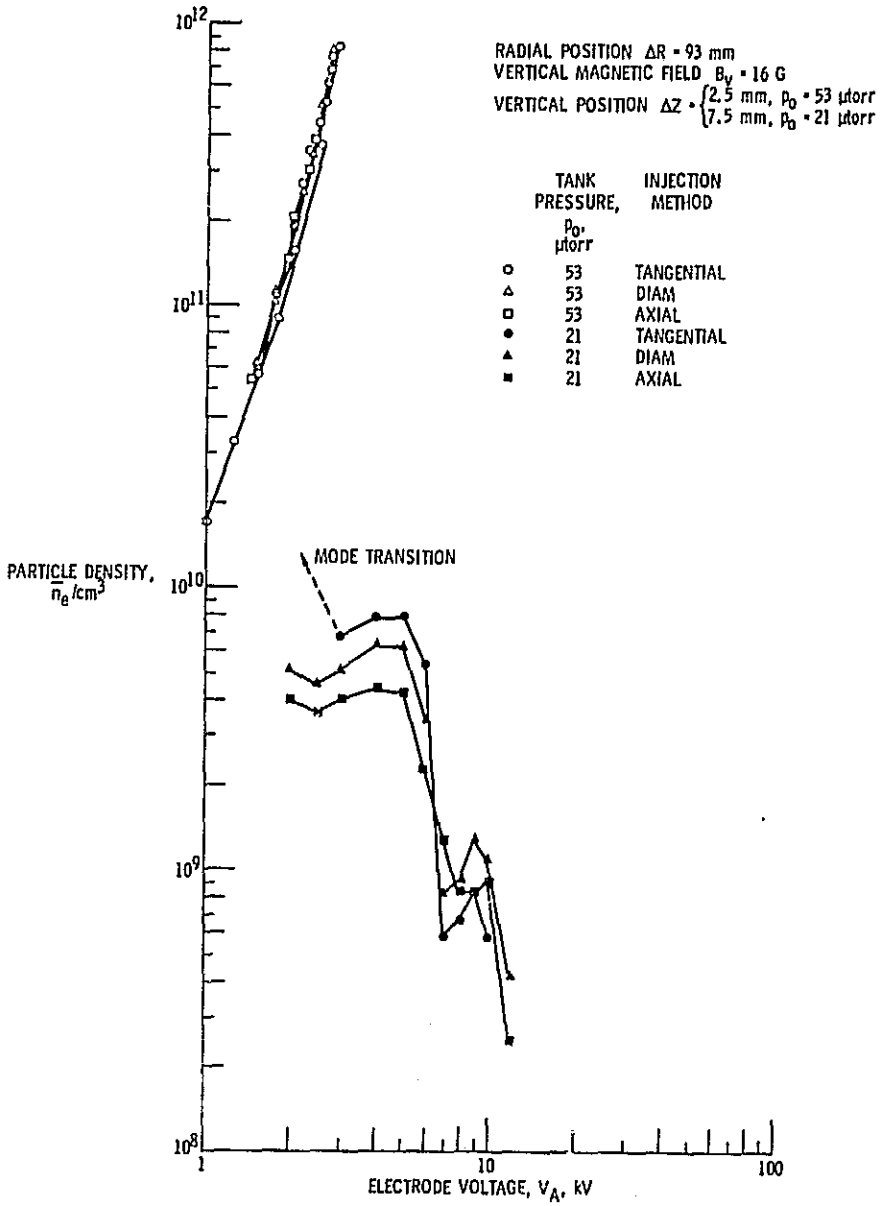

(b) NEGATIVE POLARITY.

Figure 9. - Concluded.

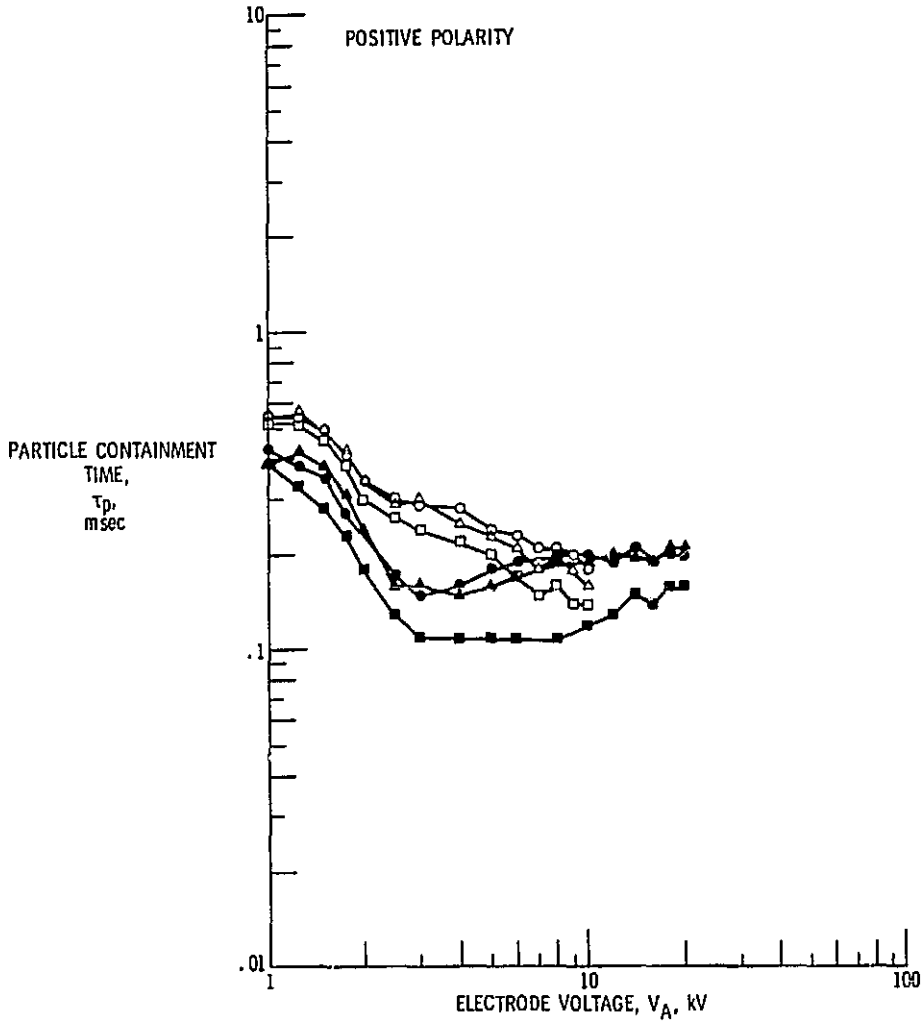

(a) POSITIVE POLARITY.

Figure 10. - Particle containment time as a function of electrode voltage for the conditions of figure 9, and for three methods of neutral gas injection.

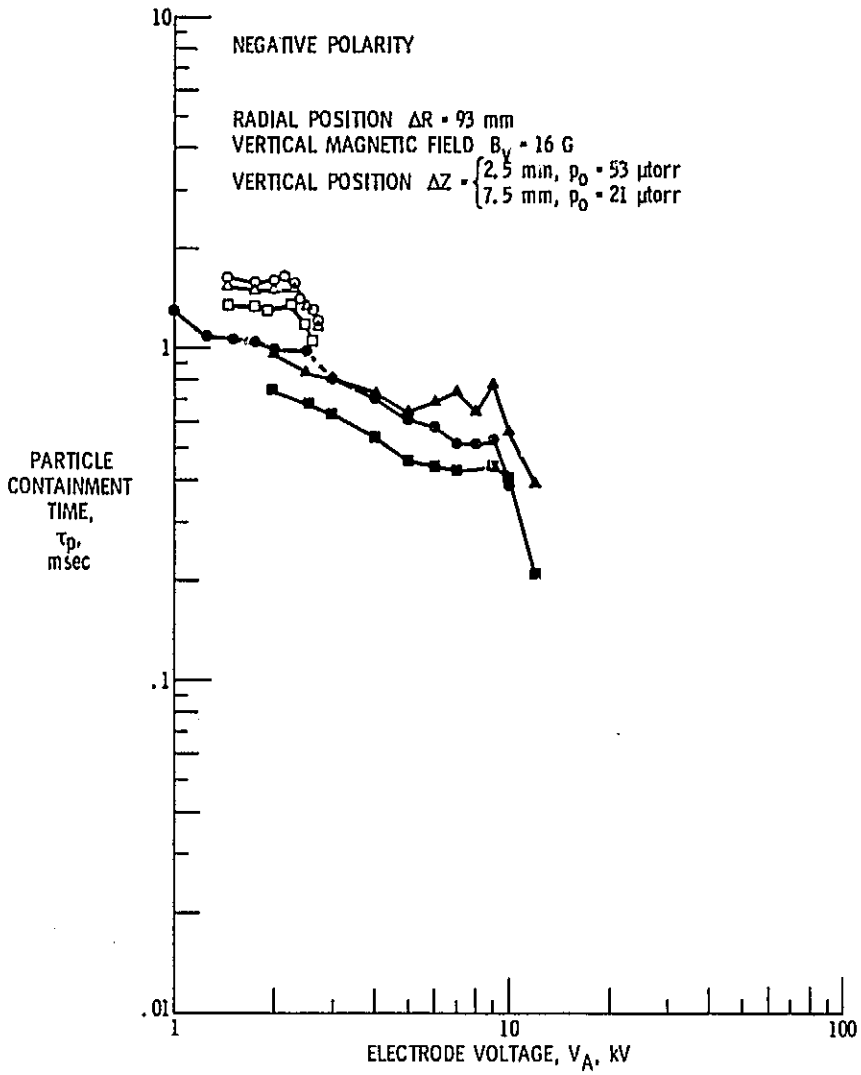

(b) NEGATIVE POLARITY.

Figure 10. - Concluded.

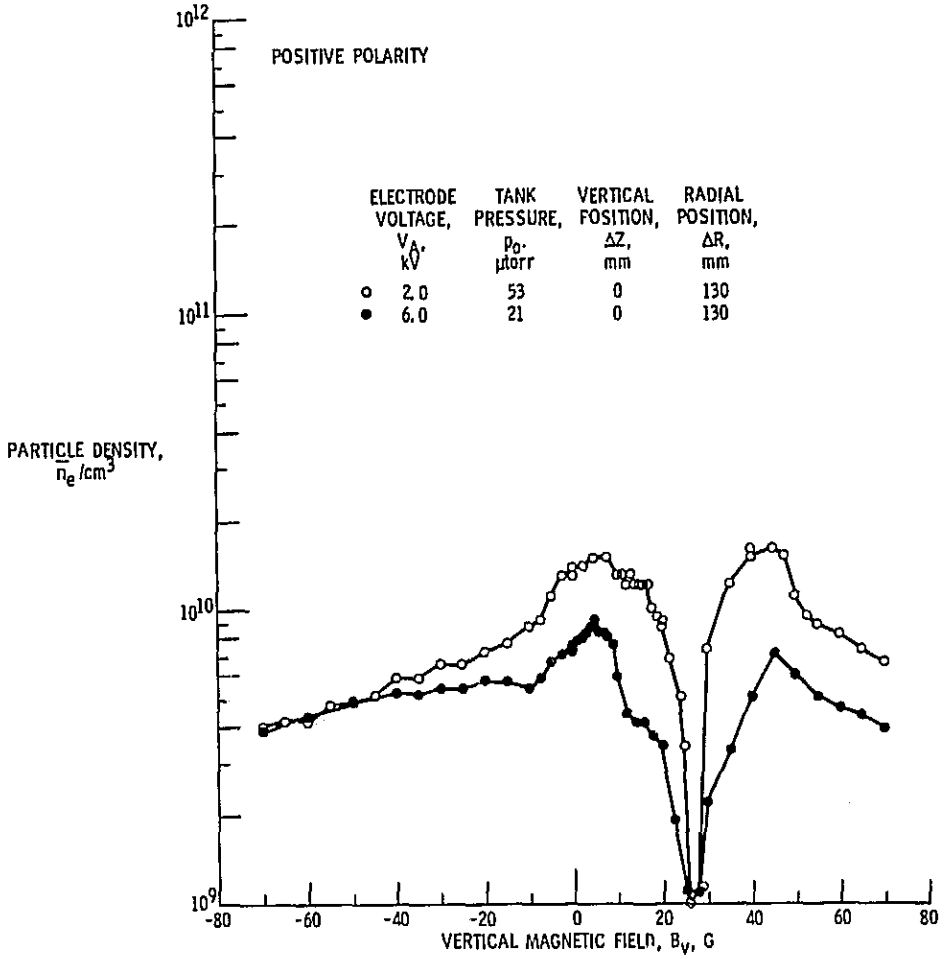

(a) POSITIVE POLARITY.

Figure 11. - Average particle number density as a function of vertical magnetic field.

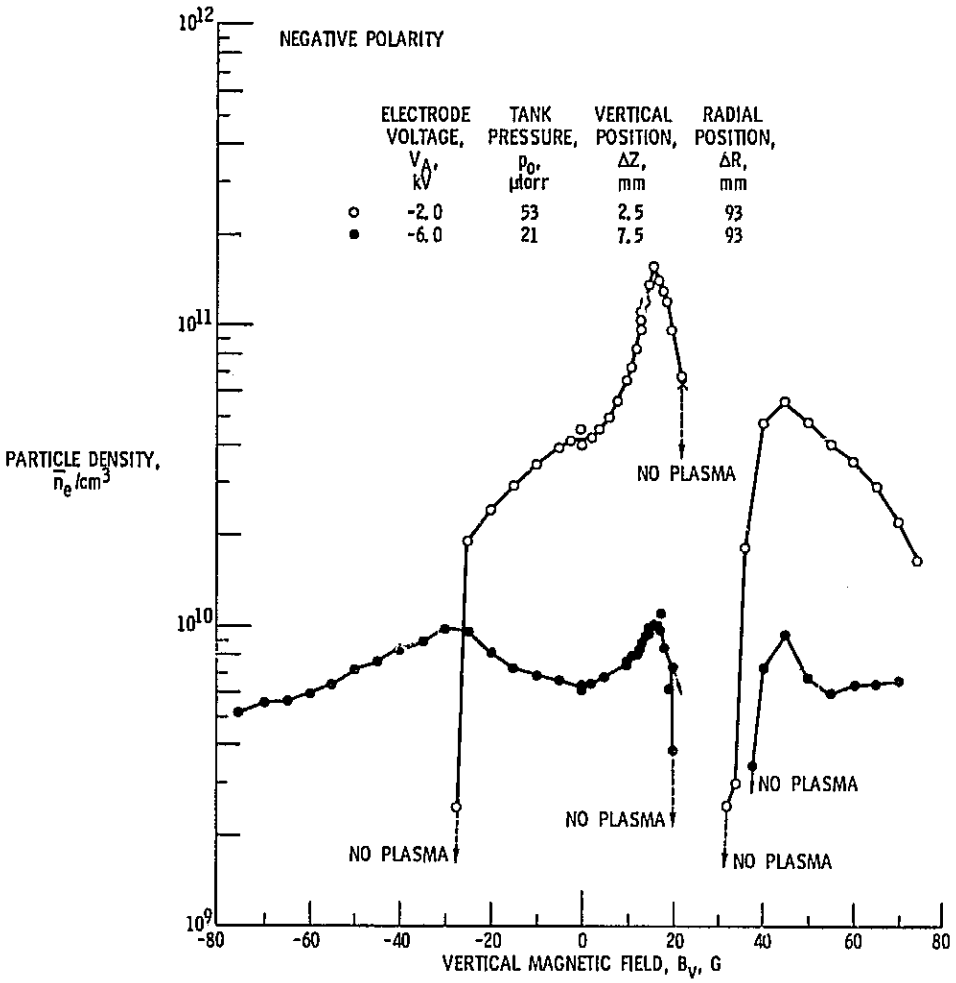

(b) NEGATIVE POLARITY.

Figure 11. - Concluded.

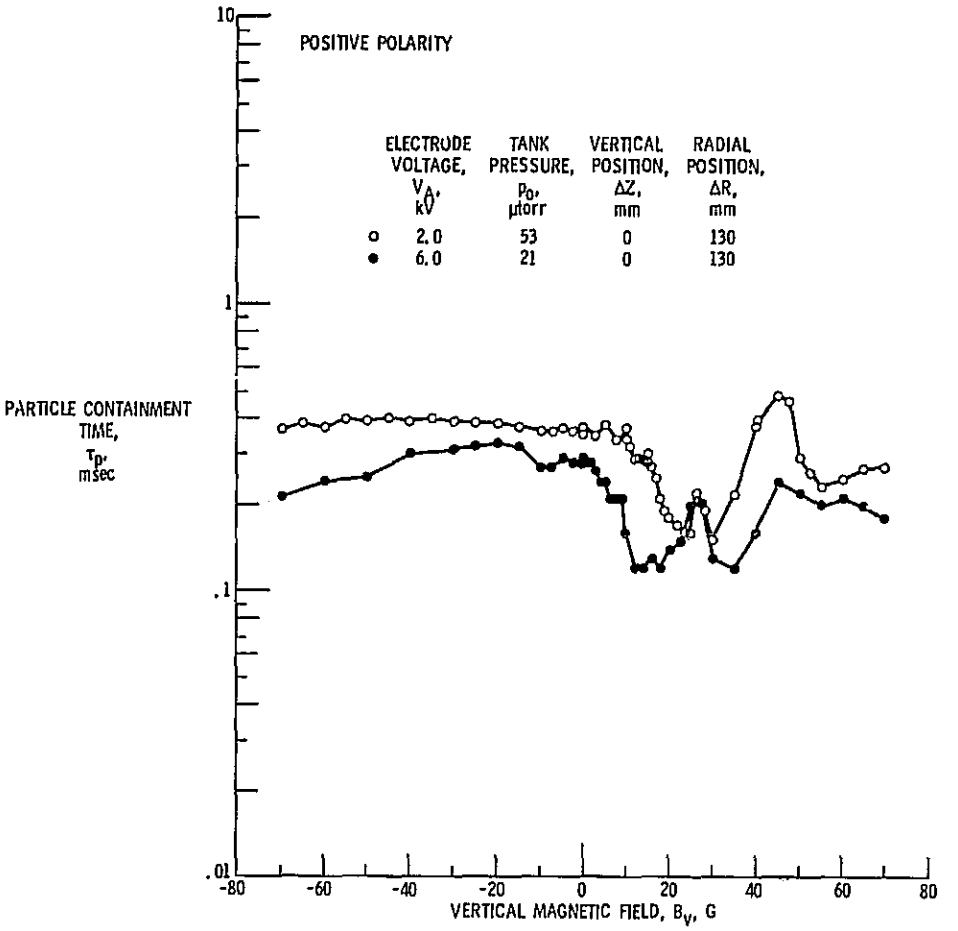

(a) POSITIVE POLARITY.

Figure 12. - Particle containment time as a function of vertical magnetic field for conditions of figure 11.

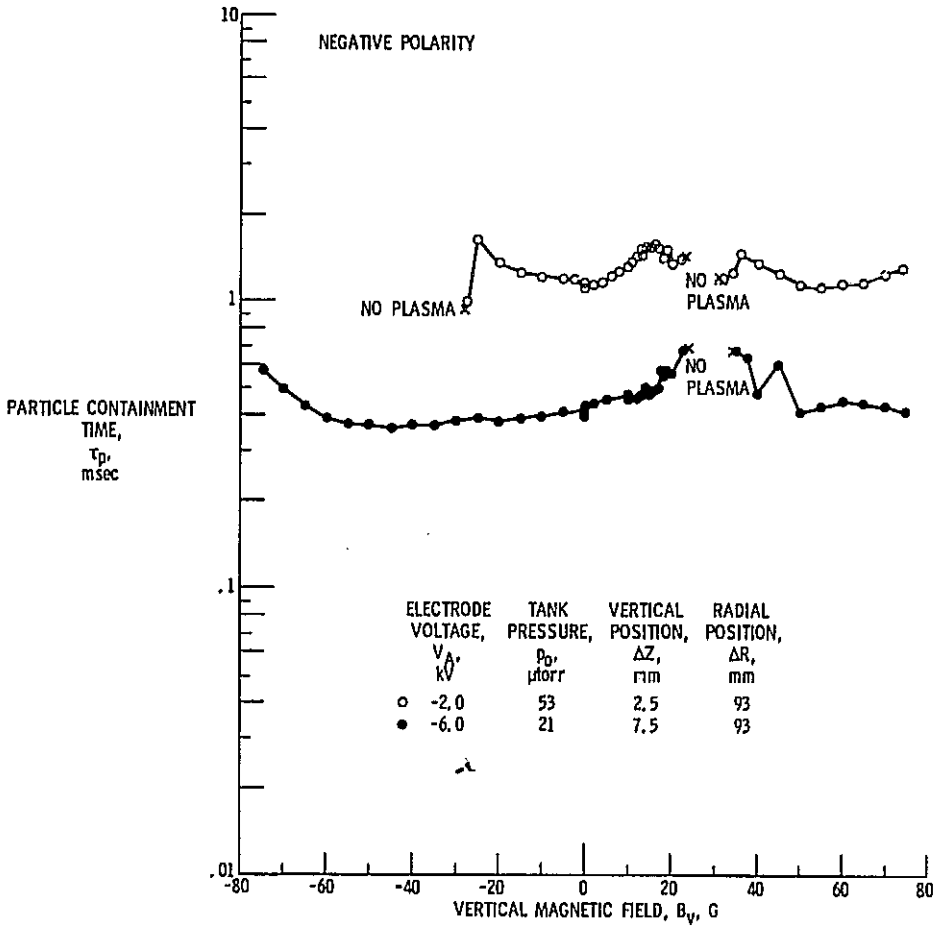

(b) NEGATIVE POLARITY.

Figure 12. - Concluded.

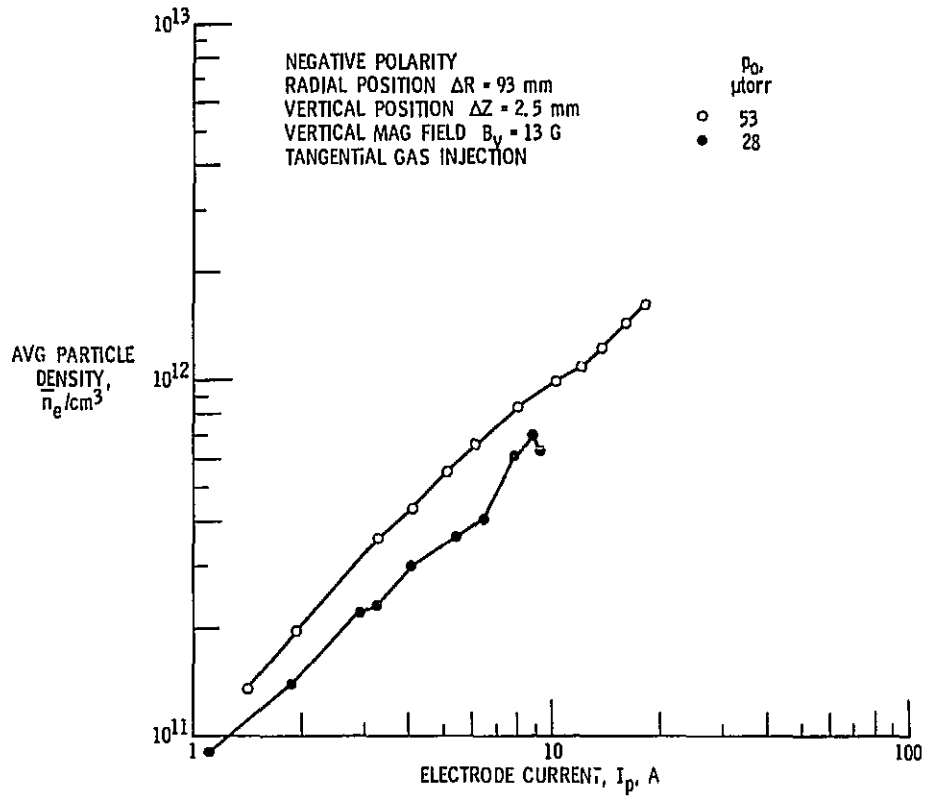

(a) PARTICLE DENSITY.

Figure 13. - Average particle density and containment time as functions of electrode current for optimized conditions.

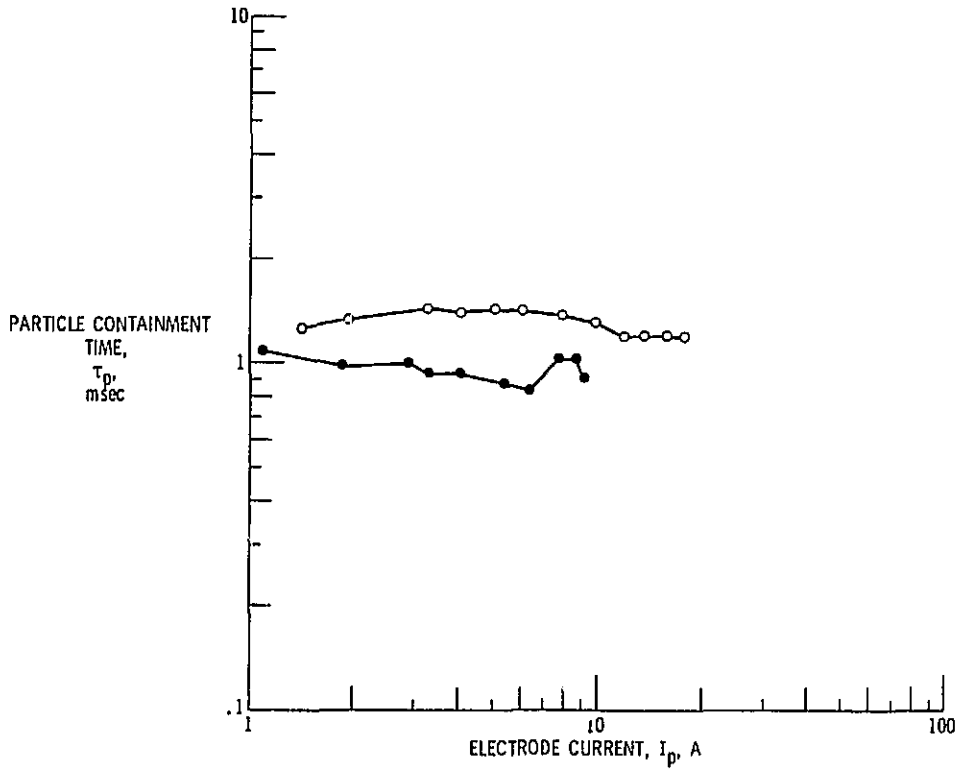

(b) CONTAINMENT TIME.

Figure 13. - Concluded.